

Double Layer Optimization Approach of Plug-in Electric Vehicle for Participation in Smart Grid Ancillary Services and Energy Markets

Mouna REKIK*[‡] , Lotfi KRICHEN** 

* Electrical Engineering Department, Electrical systems and renewable energies Laboratory (LSEER), University of Sfax, National Engineering School of Sfax (ENIS), 3038 Sfax, Tunisia

** Electrical Engineering Department, Electrical systems and renewable energies Laboratory (LSEER), University of Sfax, National Engineering School of Sfax (ENIS), 3038 Sfax, Tunisia

mouna.rekik@isimg.tn, lotfi.krichen@enis.tn

[‡]Corresponding Author; Mouna REKIK, 3038 Sfax, Tel.: (+216) 74 274 418,

Fax: (+216) 74 275 595, mouna.rekik@isimg.tn

Received: 07.06.2021 Accepted: 13.07.2021

Abstract- With the smart grid upgrade, the development of Plug-in Electric Vehicles (PEVs) is increasing exponentially thanks to their bidirectional chargers. This paper proposes a PEVs Central Controller "(PEVCC)" approach implemented for PEVs to improve power quality and participate in the electricity market. The suggested approach is divided into two optimization layers. The first one aims to estimate the optimal reference power applied to each PEV converter in order to simultaneously achieve the smoothness of utility daily power demand, the regulation of grid frequency and the minimization of daily total cost incurred for each PEV charging/discharging. The second optimization layer is designed to ameliorate the PEV dynamic by adjusting all regulators parameters during different ancillary services participating. Every optimization layer of the proposed "PEVCC" control is executed using Particle-Swarm-Optimization (PSO) algorithm. The simulation results indicate that utilizing "PEVCC" approach allows an optimal integration of PEVs into the distribution system to improve the reliability of the smart grid.

Keywords Smart grid, Plug-in Electric Vehicles, PEVs Central Controller, two optimization layers, electricity market, power quality, regulators parameters.

1. Introduction

Due to the swift growth integration of fluctuating loads in the main grid, especially during peak hours, production stress and stability problems can appear and damage the correct operation of the utility power system and consumer equipments [1,2]. To improve the future power system efficiency and mitigate environmental challenge, inventive strategies have been concentrated to raise the visibility of renewable energy field to contribute in system services and promise a suitable function of the future main grid. From these strategies, Ref. [3] proposes a power reference scheme of wind turbines for grid frequency regulation. In this work, the wind turbines active power contribution is incremented to half of power disturbance in the grid to achieve higher frequency regulation. Another control strategy dependent on

photovoltaic power availability for grid frequency enhancement is proposed in [4]. This control is based on providing frequency reserves using a frequency-watt function to adjust measured grid frequency as a function of generating photovoltaic active power. Moreover, a study in [5] interested in the grid voltage improvement, presents an experimental analysis of smart photovoltaic inverter to inject and absorb reactive power to and from the grid by means of Volt-Var control function. The combination of renewable energy sources and smart technologies presents good ideas to enhance power system stability and reduce greenhouse gas emissions. However, the irregular and fully weather-based nature of these sources, especially, with electricity demands fluctuations, present their critical barrier and handicap [6,7].

For that, to minimize renewable energy gaps and solve grid stability problems, the introduction of Plug-in Electric Vehicles (PEVs) presents the key solution for future smart grid. These electric vehicles offer obvious benefits like reducing products of oil dependency as well as pollutant gas emissions [8-10]. Moreover, with the intervention of advanced metering infrastructure, sensing technologies and bidirectional data communication flow, PEVs present a great solution to improve the energy sustainability and to achieve better economic benefits. For that, extensive research efforts focus on PEVs control strategy developments to increase the contribution of these vehicles in the ancillary services and the electricity market penetration. Indeed, Ref [11] presents two real-time dispatch strategies based on area regulation requirement and area control error to improve frequency quality. These strategies are implemented according to the charging power demands of PEVs in charging stations. Similarly, Ref. [12] proposes a cooperative centralized and distributed approach applied on PEVs and a wind power generator for coordinated frequency regulation. A comparison between droop and virtual inertia for better frequency state improvement is also discussed in this reference. The author in [13] designs a two-stage hierarchical control method based on predictive models. The main objective of this control is making PEVs abilities to replace traditional reactive power compensation devices in order to regulate grid voltage and maintain it within a desired range. For minimizing demand stress on the grid, a real-time scheduling technique applied on large-scale PEVs integrated into smart grid to reduce the peak loads demands, is proposed in [14]. Moreover, a study in [15] proposes an energy management algorithm to manage electrical vehicles power injections and absorptions in order to flatten residential loads demands of a smart city. For energy market contribution, Ref [16] investigates an approach based on model predictive control to reduce both energy generation cost and PEV charging cost in meeting both consumers and PEV power demands. Also, Ref [17] proposes an optimization framework based on hourly energy prices estimation to reduce electricity bills of a smart company equipped with wind farms and electric vehicles. Other authors as [18, 19] are interested in ameliorating the PEV dynamic response, during both charging and discharging operation concepts, by determining the optimal PID controllers' parameters. The gains of controllers are tuned using advanced optimization techniques such as stochastic fractal algorithm and multi-objective genetic algorithm. As has been presented, a wide variety of tools, techniques, and approaches have been proposed in the recent years for dealing with PEVs participating purposes in ancillary services or energy markets. However, the existing techniques still show some important gaps which have motivated this work and are indicated below:

- Each of these approaches aims at a particular objective task (grid frequency enhancement, economic benefits achievement or grid stress minimization, etc...) and, they don't solve various problems quality in power systems at the same time.

- Within previous studies, there is not enough flexibility either in PEV duration of charging or in time of connection and disconnection.
- Many of these studies apply the technology of vehicle to grid in order to ameliorate power system quality. However, they don't consider that this technology will cause a short lifetime of vehicles batteries and other unsolved issues.

The main objective of this work is filling the important gaps listed above, by developing a novel multi-objective PEVs Central Controller "(PEVCC)" approach implemented for PEVs scheduling in a smart distribution network. In this approach, various system services and economic issues as well as maximum flexibility in PEV time connection and their charge/discharge duration are simultaneously taken into consideration. Compared to previous methods, this approach can be applied to any smart grid with any number of PEVs. More precisely, the principal contributions of this work are highlighted along these lines:

- Maximization of grid frequency quality enhancement by active power dispatching between connected PEVs and smart grid.
- Minimization of the daily power demand peak intensity and achievement of a greater smart grid energy balance.
- Minimization of charging energy cost to give economic returns to PEV users.
- Detection of PEV optimal operating access to function in Vehicle-to-Grid (V2G) and Grid-to-Vehicle (G2V) concepts.
- Control of each PEV battery State Of Charge (SOC) by limiting the deep discharge " $SOC_{i,min}^{PEVc}$ " and overcharge " $SOC_{i,Max}^{PEVc}$ " in order to improve PEV battery's lifetime.
- Ensure optimal PEVs dynamic responses by adjusting all their regulators parameters during different operating concepts.

This paper is structured in this way: both of the general description of the studied system configuration and modelling of the PEV are presented in Section 2. The proposed multi-objective "PEVCC" approach to improve power effectiveness and participate in the electricity market is developed in Section 3. This approach is divided into two optimization layers that will be explained in the first and second parts of Section 3, respectively. In Sections 4 and 5, descriptions of simulation results and conclusion of this paper are detailed.

2. Description and modeling

2.1. Studied system infrastructure

The studied system architecture, as shown in Fig.1 is constituted by a smart distribution network with PEVs disposed in different area stations (Residential, Industrial and Commercial). These PEVs can behave as distributed resources or as loads in concepts known as V2G or G2V operating mode, respectively.

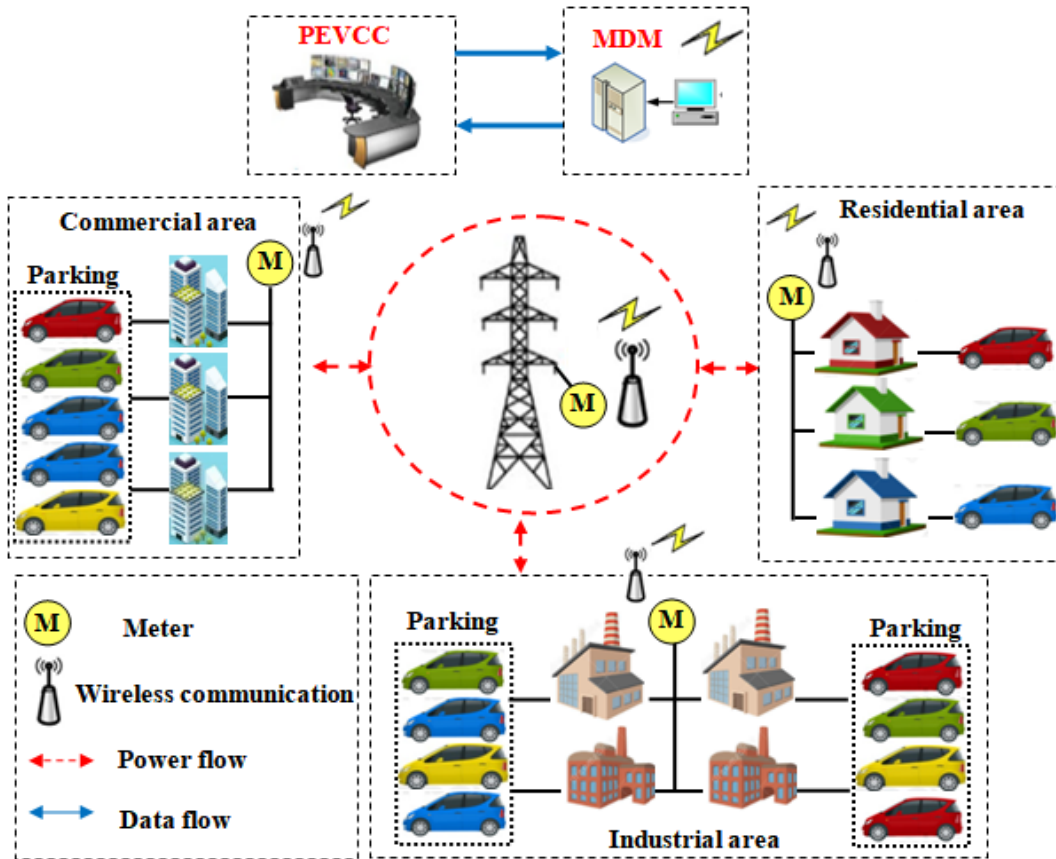


Fig. 1. Scheme of the smart-grid analyzed system.

At the top side level of studying system architecture, the "PEVCC" is sited to manage and monitor in a smart and harmonized way the communication power and data flows between PEVs and smart grid. The main objective of "PEVCC" approach is to make each PEV able to participate in system services and electricity market taking into account the PEV time connection and charge/discharge duration flexibilities. This approach is divided into two optimization layers: The first one aims to estimate the optimal reference power applied to each PEV converter in order to simultaneously achieve: the smoothness of utility daily power demand, the regulation of grid frequency, the minimization of daily total cost incurred for each PEV charging/discharging, the detection of optimal operating access of V2G or G2V concepts and the control of battery SOC for each PEV. The second optimization layer is designed to achieve optimal PEVs dynamic responses by adjusting all their regulators parameters during participating in ancillary services. In order to reach these purposes, "PEVCC" approach requires various data in real time of all studied system equipment.

For that, smart meters are installed at all the customer premises, PEV connection charging station and distribution smart grid to measure in real-time all necessary data for optimal operation. Then, they automatically send these information measurements to the Meter Data Management (MDM) system through wireless communications [20, 21]. The MDM receives and collects these data from all smart

metering systems in order to deliver them to "PEVCC" approach if needed.

2.2. Electric vehicle model and power generation control

The PEV model is generally characterized by an electric battery pack with the charging system. The Li-ion battery represents the most exploited batteries in vehicular field thanks to its safety nature, extended lifetime, high densities of energy and its lower cost [22, 23]. The Li-ion battery terminal voltage can be modulated as controlled voltage source "E_{batt}" with equivalent internal resistance "R_{L-ion}" as shown in equation (1) [24, 25]:

$$V_{L-ion} = E_{batt} - R_{L-ion} \cdot I_B \quad (1)$$

The voltage equations "E_{batt}" of Li-ion battery in charging and discharging operation are depicted in equations (2) and (3) [24, 25]:

$$E_{batt}^{ch} = V_0 - K \frac{Q}{I_{Bt} - 0.1Q} I_B^* - K \frac{Q}{Q - I_{Bt}} I_{Bt} + Ae^{-(B \cdot I_{Bt})} \quad (2)$$

$$E_{batt}^{disch} = V_0 - K \frac{Q}{Q - I_{Bt}} I_B^* - K \frac{Q}{Q - I_{Bt}} I_{Bt} + Ae^{-(B \cdot I_{Bt})} \quad (3)$$

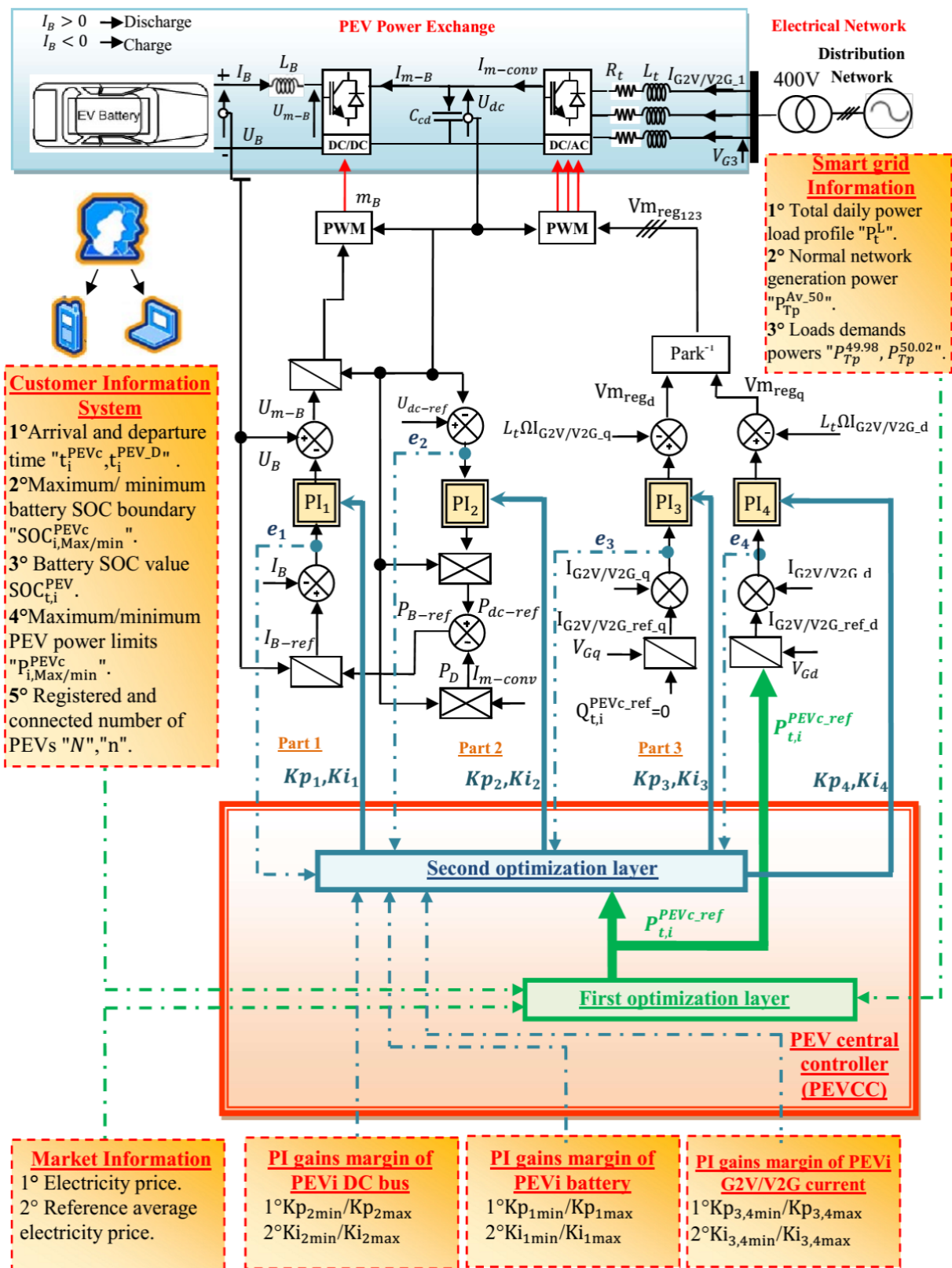


Fig. 2. PEVi control configuration for power injection/absorption.

The parameters and characteristics of Li-ion batteries implemented in studied PEVs are presented in Table 1. In addition to lithium-ion battery, each PEV contains an inductive filter and a bi-directional DC/DC converter to allow power exchanges in both charge and discharge directions and to adapt the output voltage of the battery pack to that of the continuous bus.

Moreover, a bi-directional DC/AC converter is interposed between the continuous bus and the " $R_t L_t$ " line to perform the energy transfer to the distribution network during G2V or V2G operating modes. For suitable power flow management between PEV and smart grid, the control of each bidirectional converter should be ensured. The control structure of each PEV system is summarized in Fig. 2 according to three different parts. The first part of Fig. 2 shows the battery pack control strategy, which is interested in regulating the charge or discharge current at the reference " I_{B_ref} ". An integral proportional PI_1 corrector type is used to adapt the battery current to that of the reference. The expression of this regulator is defined in equation (4):

$$U_{m_B} = U_B - PI_1 (I_{B_ref} - I_B) \tag{4}$$

The PI_1 controller gains (Kp_1, Ki_1) are estimated, at every system's new state, by the second optimization layer to decrease as maximum the target error of each PEV's battery current to zero. In order to fix the current direction for the charging or discharging phase and to adapt the modulated voltage of the battery pack to that of the continuous bus, the reversible chopper is controlled by the conversion function " m_B " as mentioned in equation (5):

$$m_B = U_{m_B} / U_{dc} \tag{5}$$

The reference current " I_{B_ref} " is calculated taking into account the reference power exchanged by the battery " P_{B_ref} " as described in equation (6):

$$I_{B_ref} = P_{B_ref} / U_B \tag{6}$$

The reference power exchanged by the battery " P_{B_ref} " is obtained by the difference between the power required to control the voltage of the continuous bus " P_{dc_ref} " and the power to satisfy the demands " P_D ", as shown in equation (7):

$$P_{B_ref} = P_D - P_{dc_ref} \tag{7}$$

Part 2 of Fig. 2 shows the continuous bus regulation block. Indeed, it is necessary to control the DC bus voltage and keep it constant, under any conditions, in order to allow a suitable power flow management between the battery pack and the continuous bus, and guarantee a balance between consumption and production. This voltage is checked by a PI_2 corrector, whose gains values (Kp_2, Ki_2) are estimated by the second optimization layer to maintain the

stored power " P_{dc_ref} " at the capacitor " C_{dc} " level equal to zero, at any new variation in the system's state. Consequently, a fast correlation of DC bus voltage to its reference is ensured.

Part 3 of Fig. 2 shows the two-way DC/AC converter control structure. The objectives of this converter are the regulation of the active and reactive power exchange between the PEV and the distribution network, besides the voltages at the " $R_t L_t$ " line terminals, during V2G or G2V operating mode.

Indeed, the supplied or absorbed currents of each PEV are regulated according to the optimum reference active powers " $P_{t,i}^{PEVc_ref}$ " calculated by the first optimization layer of proposed "PEVCC" approach and the optimum reference reactive power " $Q_{t,i}^{PEVc_ref}$ " which is equal to zero to ensure a power factor equivalent to one. These reference powers give the "d-q" components of the reference currents " $I_{G2V/V2G_ref_d}, I_{G2V/V2G_ref_q}$ " which aim to manage the transferred active and reactive powers in both V2G or G2V operating modes. Two "PI" correctors (PI_3, PI_4) are used to check the transferred currents " $I_{G2V/V2G_d}, I_{G2V/V2G_q}$ " at the connection " $R_t L_t$ " line with their references. The PIs controller gains (Kp_3, Ki_3) and (Kp_4, Ki_4) corresponding in order to the V2G/G2V currents in d and q components are estimated by the second optimization layer to reduce to the maximum, under any condition, the errors between " $I_{G2V/V2G_d}, I_{G2V/V2G_q}$ " and their references " $I_{G2V/V2G_ref_d}, I_{G2V/V2G_ref_q}$ " to zero and to also provide, at the output, the two adjustment voltages " $V_{m_reg_d}, V_{m_reg_q}$ " for the PWM inverter control.

3. Multi-objective "PEVCC" approach

For optimal integration of PEVs in the smart grid, the "PEVCC" approach is proposed to calculate, in the first step, the optimal reference power " $P_{t,i}^{PEVc_ref}$ " that should be injected or absorbed by each connected PEV to minimize each from: the daily power demand variance, the grid frequency variation and the daily total cost incurred for each PEV charging/discharging. In the second step, this approach calculates the optimal PIs controller's gains to achieve a fast PEV dynamic response during participation in these ancillary services. To ensure these goals mentioned above, the "PEVCC" receives from MDM system, in real time and during 24-h, all necessary information about the smart grid, customer's PEV, electricity market, regulators errors and gains margins as follows:

-Smart grid:

- P_t^L The total daily power load profile supplied by the grid.
- $P_{Tp}^{Av_50}$ Normal network generation power.

$P_{Tp}^{49.98}$ Loads demands power corresponding to 49.98 Hz frequency.
 $P_{Tp}^{50.02}$ Loads demands power corresponding to 50.02 Hz frequency.

-Customer's PEV:

$SOC_{i,max/min}^{PEVc}$ Maximum/ minimum battery SOC boundary of PEVi.
 $t_i^{PEVc}, t_i^{PEV_D}$ Arrival and departure time of PEVi.
 N Total number of registered PEVs in different charging station areas.
 n Total number of connected PEVs in different charging station areas.
 $P_{i,max/min}^{PEVc}$ Maximum/minimum limits of each PEV charging-discharging power.
 W_i^{PEV} Initial charge of PEVi battery at connection to the charging station.
 Q_i^{PEV} Capacity of connected PEVi battery.
 η_i^{PEV} Efficiency of connected PEVi battery.
 AD^{PEV_D} Course distance by the customer's PEV .

-Electricity market:

$Cost_t$ Electricity price at time t.
 $Cost_{avr_Tp}$ Reference average electricity price during Δt_p .

-PIs gains margin:

Kp_{1min}/Kp_{1max} PI gains margins information of each PEV battery current.
 Ki_{1min}/Ki_{1max}
 Kp_{2min}/Kp_{2max} PI gains margins information of each PEV DC bus.
 Ki_{2min}/Ki_{2max}
 Kp_{3min}/Kp_{3max} PI gains margins information of each PEV G2V/V2G current in q axes.
 Ki_{3min}/Ki_{3max}
 Kp_{4min}/Kp_{4max} PI gains margins information of each PEV G2V/V2G current in d axes.
 Ki_{4min}/Ki_{4max}

-PIs instantaneous errors:

$e1$ PI error information of each PEV battery current.
 $e2$ PI error information of each PEV DC bus.
 $e3$ PI error information of each PEV G2V/V2G current in q axes.
 $e4$ PI error margins information of each PEV G2V/V2G current in d axes.

It is noted that the "PEVCC" approach can be applied to any smart grid with any number of PEVs. Moreover, this approach takes into consideration, simultaneously and at maximum, the flexibility in PEV time of connection and disconnection, the battery SOC in the connection time and its charge/discharge duration. The proposed "PEVCC" approach

contains two essential layers. The mathematical formulation and the multi-objective optimization of these layers will be described in detail in the next sub-sections.

3.1. Problem formulation and constraints of the first optimization layer

The consequence of active power mismatches between the grid supply and load variance demand causes a fluctuation in the system frequency. In fact, the extra demand builds to frequency drop and the deficit demand builds to frequency increase [26,27]. Grid codes specify that frequency variation range should be between 49.98 Hz and 50.02 Hz, and, operation beyond these borders would damage the electrical network equipments [28]. For that, equilibrium between active power produced and consumed must be preserved in spite of load demands changing. To minimize as much as possible the supply-demand inequality and obtain a flat daily power demand with grid frequency convergence to nominal value 50 Hz, in this paper, the studied PEVs operate in G2V or V2G concepts to absorb or inject the optimal active power determined by the first optimization layer of "PEVCC" approach. The problem function can be formulated as equation (8):

$$P_{Tp}^{50.02} \leq \left(P_t^L + \sum_{i=1}^n P_{t,i}^{PEVc_ref} \right) \leq P_{Tp}^{49.98} \tag{8}$$

With:

$$\begin{cases} t=1 \dots Tp \\ i=1 \dots n \\ n=1 \dots N \end{cases}$$

The one-day cycle (24-hour) is divided into Tp time-periods, with the duration of each one is fixed by $\Delta t_p = 15$ min. So, 96 periods are obtained through one day. The control is achieved here by calculating the optimal reference active power " $P_{t,i}^{PEVc_ref}$ " of each PEVi connected to different station areas. This reference power is injected or absorbed into or from the grid, respectively, in order to flatten the total load power " P_t^L " to coincide, as much as possible, with the normal network generation " $P_{Tp}^{50.02}$ " corresponding to the 50 Hz frequency. At each Δt_p period, the priority order of PEVs services is classified according to the first PEV connection time detected by the smart meter. The proposed approach is flexible to join any PEVs number with any connection and disconnection time. The calculated references active powers applied on PEVs converters are optimal because they consider many constraints at the same time:

- **Constraint 1:** The reference active power exchanged

" $\sum_{i=1}^n P_{t,i}^{PEVc_ref}$ " between connected PEVs and the grid must be insured according to definite standards, without troubling the electrical network stability and to maintain the

frequency state in the norm range [49.98, 50.02 Hz]. For that, the sum of both total load power and all connected PEVs charging/discharging power must be within the maximum and minimum limits of loads demands power corresponding in order to 49.98 Hz and 50.02 Hz grid frequency, as described in equation (9):

$$P_{Tp}^{50.02} \leq \left(P_t^L + \sum_{i=1}^n P_{t,i}^{PEVc_ref} \right) \leq P_{Tp}^{49.98} \quad (9)$$

- **Constraint 2:** The technologies of Li-ion batteries have incrementally advanced in the large PEVs market. The battery SOC illustrates the significant parameter to indicate the charge-discharge level of a PEV battery storage system during connection or disconnection to the charging station. The accurate control of over charge and deep discharge states improves the long lifespan, efficiency and safety of PEV battery [29]. For that, in this paper the first optimization layer of "PEVCC" approach is also interested in upgrading the PEVs batteries functionality and robustness by limiting the SOC as indicated in the constraint expressed by equation (10):

$$\begin{cases} SOC_{i,min}^{PEVc} \leq SOC_{t,i}^{PEV} \leq SOC_{i,max}^{PEVc} \left(t = t_i^{PEVc} \square t_i^{PEVd} \right) \\ SOC_{i,min}^{PEV} \leq SOC_{t,i}^{PEV} \leq SOC_{i,max}^{PEVc} \left(t = t_i^{PEVd} \square t_i^{PEVc} \right) \\ SOC_{i,min}^{PEV} < SOC_{i,min}^{PEVc} \end{cases} \quad (10)$$

Two values of minimal battery SOC are considered in this paper: one is the deep discharge during participating in the ancillary services "SOC_{i,min}^{PEVc}" and the second corresponds to the deep discharge during PEV traveling "SOC_{i,min}^{PEV}". In fact, PEV may inject power to the grid in the process of V2G operation concept by taking into account the battery energy reserve for disconnection and departure flexibility. The mathematical expressions of electric vehicles Li-ion battery SOC at PEV instant of connection into the charging station "t_i^{PEVc}" and during the length of connecting time-period "(t_i^{PEVc} □ t_i^{PEVd})" are shown in order by equations (11) and (12) [15, 30]. During disconnection time-period depends on the storage, the PEV battery "(t_i^{PEVd} □ t_i^{PEVc})" course distance "AD^{PEV_D}" of every PEV traveling and on the vehicle efficiency "η_i^{PEV}". The required energy "P_{tr}^{PEV_D}" needed for PEV trip is described in equation (13) [15]:

$$SOC_{t,i}^{PEV} = \begin{cases} \frac{W_i^{PEV} + P_{t,i}^{PEVc} \cdot \eta_i^{PEV} \cdot \Delta t_p}{Q_i^{PEV}} \left(t = t_i^{PEVc} \right) & (11) \\ SOC_{t-1,i}^{PEV} + \frac{P_{t,i}^{PEVc} \cdot \eta_i^{PEV} \cdot \Delta t_p}{Q_i^{PEV}} \left(t = t_i^{PEVc} \square t_i^{PEVd} \right) & (12) \end{cases}$$

$$\begin{aligned} 0 < \eta_i^{PEV} < 1 \\ P_{tr}^{PEV_D} = \eta_i^{PEV} \cdot AD^{PEV_D} \end{aligned} \quad (13)$$

It is noted that all these parameters are measured and detected by means of smart meters, when the PEV is connected at the charging station.

- **Constraint 3:** In favor of durable operation of PEV battery storage, the exchanged power between each connected PEV and smart grid, during V2G or G2V concepts, should be restricted by a definite maximum and minimum level. For that, the first optimization layer of "PEVCC" approach limits each PEV charging-discharging power as shown in equation (14):

$$P_{i,min}^{PEVc} \leq P_{t,i}^{PEVc} \leq P_{i,max}^{PEVc} \quad (14)$$

- **Constraint 4:** Due to significant PEVs penetration along the electrical grid, they have an appreciated potentiality in the energy market. In this work, the vehicles contribution in the energy market appeared in charging cost minimization. PEVs connected to the different charging station areas absorb and inject energy from and to grid during operation in G2V or V2G concepts, respectively. In both operating concepts, the energy cost changes according to power consumption levels. It is expensive during periods of high demand and cheaper during periods of low demand. For that, the PEVs' owners should as much as possible discharge their electric vehicles at high- price and charge them when electricity cost is the cheapest. In this case, an optimal buying and selling energy for PEVs' owners is obtained. The constraint of charging cost minimization by optimal bidding is described as equation (15):

$$\min \sum_{t=1}^{Tp} P_{t,i}^{PEVc} \cdot (Cost_t - Cost_{avr_Tp}) \quad (15)$$

In accordance with the position of actual energy price "Cost_t" relative to the reference average electricity price "Cost_{avr_Tp}", this constraint guarantees an optimal power exchange "P_{t,i}^{PEVc}" between each connected vehicle and smart grid in order to raise revenue and money earn to PEV users during both G2V/V2G operation concepts. In fact, the G2V operation is available only when "Cost_t" is less than "Cost_{avr_Tp}". On the other hand, the V2G operation is allowed during the high price energy characterized by "Cost_t" higher than "Cost_{avr_Tp}".

3.2. Problem formulation and constraints of the second optimization layer

After estimation of the optimal references active power " $P_{t,i}^{PEVc_ref}$ " applied to each PEV converter to simultaneously achieve: the smoothness of utility daily power demand, the regulation of grid frequency and the minimization of daily total cost incurred for each PEV charging/discharging, the second optimization layer is designed to adjust all regulators parameters during different operating modes to ameliorate the PEV dynamic response and guarantee an optimal convergence of the measured PEV injected power " $P_{t,i}^{PEVc}$ " to the reference one estimated by the first optimization layer " $P_{t,i}^{PEVc_ref}$ ". In fact, a novel external perturbation may have an impact on the PEV system stability and response quality which is essentially linked to the regulator parameters. In this case, the four PI controller's gains of each PEV, corresponding to DC bus voltage " U_{dc} ", battery current " I_B " and G2V/V2G absorbed/ injected current in both axes d,q " $I_{G2V/V2G_d}, I_{G2V/V2G_q}$ ", should be variable and adjustable when a new variation is accrued in the system. For this reason, the second optimization layer is based on finding the optimal controller parameters, at every system's new state, to decrease to the maximum the target error of each PEV's [" U_{dc} ", " I_B ", " $I_{G2V/V2G_d}$ " and " $I_{G2V/V2G_q}$ "] to zero with a short time. Consequently, an adequate regulation to the PEV injected power at its desired value is guaranteed. To achieve the goals mentioned above, the mathematical function to be optimized is the Integral Time Absolute Error "ITAE" technique defined in equation (16). This technique is adopted in the second optimization layer because it accomplishes the lowest error indexes with smaller oscillations and overshoots compared to the other fitness techniques [31, 32].

$$\min \{f_t(k) = ITAE_t(k)\}$$

$$ITAE_t(k) = \int t |e_k(t)| dt \quad (16)$$

$$k = 1 : 4$$

The second optimization layer receives, in the first step, as data input, the errors " $e_k(t)$ " and the gains constraints of each PEV's [" U_{dc} ", " I_B ", " $I_{G2V/V2G_d}$ " and " $I_{G2V/V2G_q}$ "] regulators PI_k with ($k = 1 : 4$). Then it minimizes every " $ITAE_t(k)$ " using the on-line multi-objective PSO algorithm which transmits as data output the optimal PI_k 's gains " Kp_k " and " Ki_k " corresponding to the minimum fitness function " $ITAE_t(k)$ ". The advanced PSO algorithm is described in detail in the subsequent subsection. The four regulators of each PEV are optimized simultaneously according to the following constraints:

- Constraint on the battery current regulator gains (PI_1) given by equation (17):

$$\begin{cases} Kp_{1min} \leq Kp_1 \leq Kp_{1max} \\ Ki_{1min} \leq Ki_1 \leq Ki_{1max} \end{cases} \quad (17)$$

- Constraint on the DC bus voltage regulator gains (PI_2) given by equation (18):

$$\begin{cases} Kp_{2min} \leq Kp_2 \leq Kp_{2max} \\ Ki_{2min} \leq Ki_2 \leq Ki_{2max} \end{cases} \quad (18)$$

- Constraint on the q-axes G2V/V2G current regulator gains (PI_3) given by equation (19):

$$\begin{cases} Kp_{3min} \leq Kp_3 \leq Kp_{3max} \\ Ki_{3min} \leq Ki_3 \leq Ki_{3max} \end{cases} \quad (19)$$

- Constraint on the d-axes G2V/V2G current regulator gains (PI_4) given by equation (20):

$$\begin{cases} Kp_{4min} \leq Kp_4 \leq Kp_{4max} \\ Ki_{4min} \leq Ki_4 \leq Ki_{4max} \end{cases} \quad (20)$$

Every proportional and integral gain " Kp_k " and " Ki_k " of each PI_k with ($k = 1 : 4$) is chosen within a well selected search space characterized by a superior and minor boundaries [" Kp_{kmin} ", " Kp_{kmax} "] and [" Ki_{kmin} ", " Ki_{kmax} "], respectively. The couple of gains are revised and adjusted on-line and at every system's new state by using the multi-objective PSO algorithm to guarantee an optimal regulation and minimum errors between measurement and reference of DC bus voltage " U_{dc} ", battery current " I_B " and G2V/V2G absorbed/ injected current in both axes d,q " $I_{G2V/V2G_d}, I_{G2V/V2G_q}$ " of each PEV. Consequently, they ensure the vehicle dynamic enhancement during participating in the ancillary services.

3.3. Implementation of the "PEVCC" approach

The two optimization layers of proposed "PEVCC" approach are implemented sequentially, one after the other. The first optimization layer is executed, in the first step, using PSO algorithm to estimate the reference optimal power " $P_{t,i}^{PEVc_ref}$ " that should be injected by each PEV. Thereafter, the second layer of optimization is executed, in the second step, to correlate this reference to the measured one " $P_{t,i}^{PEVc}$ " by calculating the optimal regulators gains, at every system's new state, by means of an on-line multi-objective PSO algorithm [33-34]. The PSO is an optimization algorithm inspired by the intelligent attitude of

fish and swarm during the discovery of their best nutritious place. It is reaching, at the present time, more attention to execute and solve various supervision problems with numerous variables due to its robustness, efficiency, simplicity and short-computation times [35]. In PSO technique, each particle travels to its best local solution " P_{Loc} " that it has discovered. Then, it communicates with its neighborhoods about this found solution and, therefore, it reviews its own velocity and position to get the best global solution " P_{Glob} ". The particle velocities are manipulated based on equations (21) and (22) [36]:

$$\Delta v(j+1) = w \Delta v(j) + R_1 C_1 (P_{Loc}(j) - v(j)) + R_2 C_2 (P_{Glob}(j) - v(j)) \quad (21)$$

$$v(j+1) = v(j) + \Delta v(j+1) \quad (22)$$

Where " $\Delta v(j)$ " and " $v(j)$ " are, in order, the velocity and the position of the particle at iteration " (j) ", " (C_1, C_2) " are the acceleration coefficients that their summation has to be less than 4, " (R_1, R_2) " illustrate the random variables that are within $[0,1]$ and " w " represents the inertia weight.

4. Results and analysis

To validate the efficacy of proposed "PEVCC" approach based on double-layered optimization, a case study constituted by 2250 PEVs distributed on four station areas is implemented by MATLAB Simulink environment according to the system parameters provided in Table 1. This approach is evaluated during 24-hours with different states of PEVs connection/disconnection times, initial batteries SOC and charge/discharge duration periods. To improve the simulation rapidity with significant number of PEVs, the identical behavior type vehicles are aggregated into one equivalent PEV. For that, in this studied case, three PEVs aggregate models are considered whose basic features are specified in Table 2. The simulation analyses to prove the robustness and the flexibility of the double-layered optimization of "PEVCC" approach are carried out in the next subsections.

4.1. First optimization layer simulation results

The first optimization layer of proposed "PEVCC" approach has been solved over a 24-h time horizon with a 15-min resolution. Consequently, the simulations present 96 periods in the day. At the beginning, the PEVs are not joined to the smart grid. The variable demanded loads are just delivered by the electrical network. Its respective total active power is depicted in Fig.3.a. The effect of these demands on the electrical frequency is well perceptible in Fig.3.b. In fact, the extra demand builds to frequency drop, and the deficit demand builds to frequency increase. Grid codes specify that frequency variation range should be between 49.98 Hz and 50.02 Hz not to harm the electrical appliances. For that, smoothness of consumed active power to the nominal grid

generation equivalent to 50 Hz of frequency must be preserved at each instant.

Table 1

Parameters of studied lithium-ion battery cell: (3.3V; 2.3 Ah).

Characteristics	Value
B	$26.5487(Ah)^{-1}$
V_0	3.366V
R_{L-ion}	0.01Ω
A	0.26422V
K	0.0076Ω

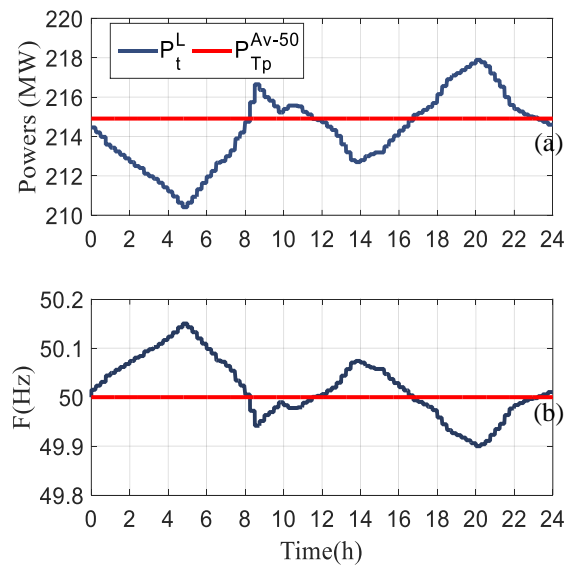


Fig. 3. Electrical grid behavior before "PEVCC" insertion: (a) Daily loads demands; (b) Grid frequency.

To achieve, as much as possible, the supply-demand equality and to flatten the daily power demand with grid frequency convergence to nominal value 50Hz, the three PEVs aggregations operate in G2V or V2G concepts into the distribution system to absorb or inject the optimal active power determined by the first optimization layer of "PEVCC" approach. The total numbers of connected vehicles in all charging station areas, as well as, the connection and disconnection times of the three PEVs aggregations (PEV_{AG1}, PEV_{AG2} and PEV_{AG3}) are shown in Fig.4.a, Fig.4.b, Fig.4.c and Fig.4.d, respectively. The priority order of PEV_{AGi} injection or absorption power is classified according to the first PEV_{AGi} connection time. The red, green and blue shaded surfaces indicate in order the first, second and last order of

priority of each PEV_{AGi} . When the vehicle disconnects from the charging station, it loses its priority order and consequently the second connected vehicle becomes prioritized the first. As shown, PEV_{AG1} is connected at the following intervals [0-3.30h], [4.30-8h] and [13-23h]. During

[3.30-4.30h], [8-13h] and [23-0h], this vehicle is not available to join the smart grid.

Table 2

Identifications of PEVs aggregations and information about concerned vehicles in the case study.

$PEVs_{AGi}$	PEV model	PEVs Registered numbers	Battery capacity Q_i^{PEV} (kWh)	$P_{i,min}^{PEVc}$ (kW)	$P_{i,Max}^{PEVc}$ (kW)	$SOC_{i,min}^{PEV}$	$SOC_{i,min}^{PEVc}$	$SOC_{i,Max}^{PEVc}$	η_i^{PEV} (%)
$PEVs_{AG1}$	Mitsubishi Outlander PHEV	500	13.8	-2	2	0.2	0.5	0.8	0.9
$PEVs_{AG2}$	Nissan Leaf	1000	14	-2	2	0.2	0.5	0.8	0.92
$PEVs_{AG3}$	Peugeot ION	750	14.5	-2	2	0.2	0.5	0.8	0.95

PEV_{AG2} is available to operate in V2G /G2V concepts for both periods of time [0.45-10h] and [14-22.30h]. In the course of these intervals [10-14h] and [22.30-0.45h], this vehicle is disjointed. PEV_{AG3} is accessible for a two-flow transfer power during [3-8.15h] and [10-21h]. Outside these periods, this vehicle is unplugged.

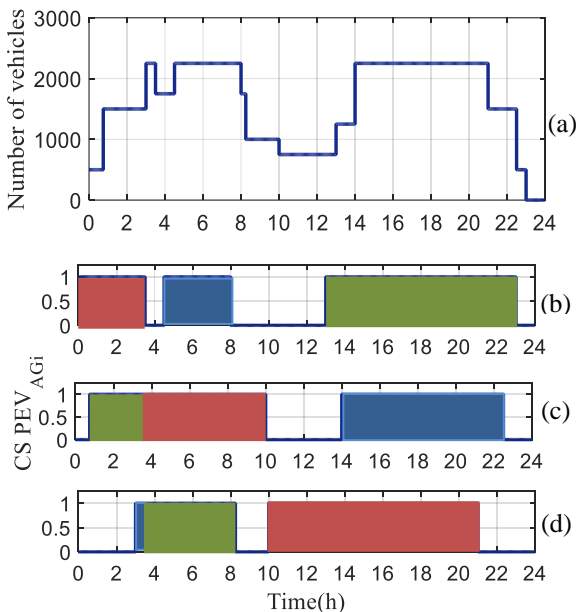


Fig. 4. Connection status of each PEV_{AGi} : (a) Number of connected vehicles. (b) PEV_{AG1} state connection. (c) PEV_{AG2} state connection. (d) PEV_{AG3} state connection.

The electricity prices indications used in this case study are shown in Fig. 5. This curve shows that the price of electricity is low during midnight and high in the morning and evening, which encourages PEVs owners to contribute to the energy market to minimize charging cost and raise revenue and money earn during both PEVs G2V/V2G operation concepts.

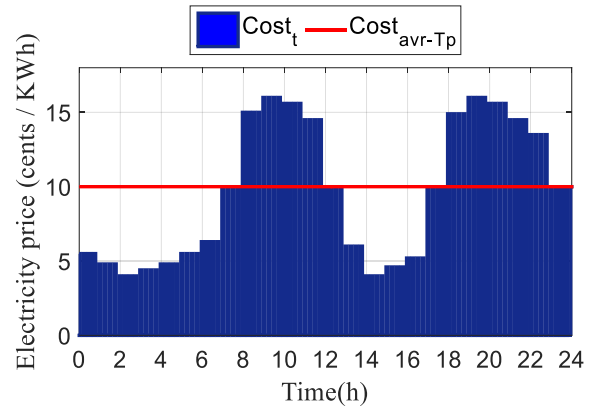


Fig. 5. Electricity prices curve.

Fig. 6 shows the PEV_{AG1} , PEV_{AG2} and PEV_{AG3} references active powers over the 96 time periods. It is clear that the negative powers present the operation of the PEVs charge known by the G2V concepts. The positive powers affirm the discharge operation known by the V2G concepts. These reference active power curves are calculated by the first optimization layer of "PEVCC" approach using the on-line multi-objective PSO algorithm with parameters shown in Table 3. They are the best solutions of the studied objectives function which consider many constraints at the same time. In fact, the difference between both total load power and normal network generation power corresponding to the 50 Hz of frequency is absorbed or injected in an optimal manner by all connected PEV_{AGi} according to:

- The actual energy price " $Cost_t$ " state. In fact, the charge is available only when " $Cost_t$ " is less than " $Cost_{avr_Tp}$ ". On the other hand, the discharge operation is allowed during the high price energy characterized by " $Cost_t$ " higher than " $Cost_{avr_Tp}$ ".

- The battery SOC of each PEV_{AGi} which should be within " $SOC_{i,Max}^{PEVc}$ " and " $SOC_{i,min}^{PEVc}$ " during charging and discharging operation.
- The PEV_{AGi} charging-discharging power which does not exceed its limits " $P_{i,Max/min}^{PEVc}$ ".

It is remarkable from Fig. 6 that the G2V concept is carried out during [0-8h] and [12-16.45h] when electricity price is low and there is a drop in the total required power. The total reference active power during these periods is the difference between " P_t^L " and " $P_{Tp}^{Av,50}$ " to flatten the daily load curve and correlate the frequency to 50 Hz. Then this total reference is distributed on every PEV_{AGi} according to their priority, over-charge, and maximum absorption power. In the course of subsequent intervals [8.15-11.30h] and [17-23h], the demand power is superior to the average power corresponding to the 50 Hz of frequency and the electricity price is expensive. This is the case of V2G concepts when the total reference active power of all connected PEVs is corresponding to the difference between the required daily power and the reference power " $P_{Tp}^{Av,50}$ " to reduce peak power, maximize PEV's owner earn revenue and enhance the frequency to be equivalent to 50 Hz. This total reference is diffused on every PEV_{AGi} according to their priority, deep discharge and maximum injection power. However, it is also observable from Fig. 6 that during the intervals [8-8.15h], [11.30-12h] and [16.45-17h], the reference powers of all connected vehicles are equal to zero. So, no PEVs transfer power to the smart grid will be ensured. Because either the load demands are lower than " $P_{Tp}^{Av,50}$ " but the electricity price is expensive or the total load demand is more than " $P_{Tp}^{Av,50}$ " but the electricity price is cheaper. It is noted that, the reference powers of each PEV_{AGi} is also equal to zero when it is not plugged to the post charge or it is connected but its SOC state attains its deep discharge " $SOC_{i,min}^{PEVc}$ " or over charge " $SOC_{i,Max}^{PEVc}$ " during operating in V2G or G2V concepts.

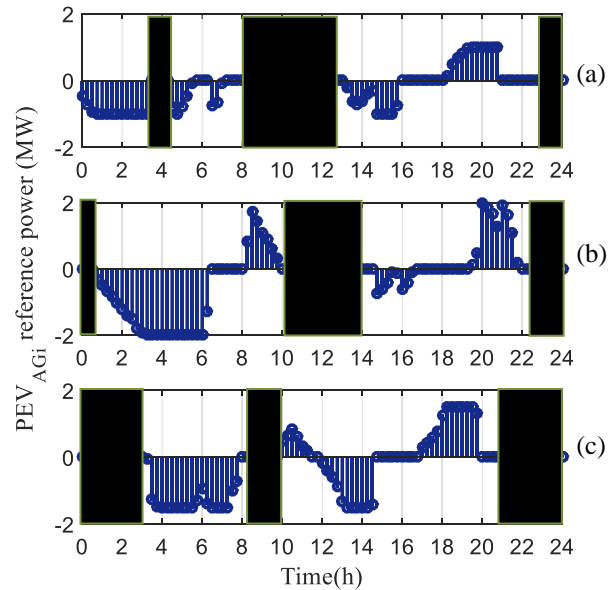


Fig. 6. PEV_{AGs} reference active powers profiles: (a) For PEV_{AG1}. (b) For PEV_{AG2}. (c) For PEV_{AG3}.

The performance of the first optimization layer tuned by the PSO algorithm to calculate the optimal reference active power of each connected PEV_{AGi}, is summarized in the fitness function presented in Fig.7. This fitness function is a combination of the studied objectives function and a penalty function to guide executions towards best design solutions during both V2G and G2V operating concepts. The convergence to the optimal value is attained after 40 iterations. It can be observed that during some periods, the fitness function is equal to zero, meaning that the objective function of the first optimization layer is attained and its constraints are all satisfied. But sometimes, the fitness function is different from zero, meaning that the best found solution is partial or doesn't reach the set aims for one or more reasons: deep discharge or over charge attainment of PEV's batteries, not enough PEVs plugged to post charge, expensive electricity price with low load demands or cheaper electricity price with peak loads demands.

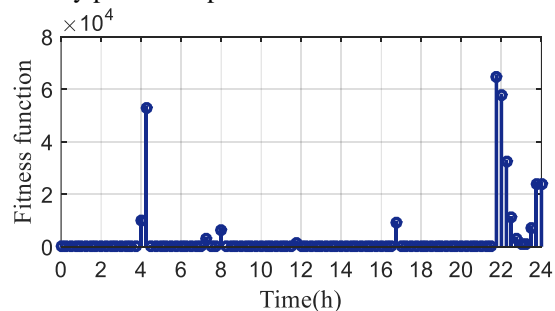


Fig. 7. Evolution of the fitness function.

4.2. Second optimization layer simulation results

After each PEV_{AGi} optimal reference active power calculation during the 96 time periods of the day, the second optimization layer is designed to adjust, simultaneously, all regulators parameters of each PEV_{AGi} connected to the post charge by means of on-line multi-objective PSO algorithm

with parameters shown in Table 3. This adjustment is ensured at every system's new state to guarantee an optimal convergence of the measured PEV_{AGi} injected power to the reference one estimated by the first optimization layer. It is noted that at every Δt_p time-periods, the estimated reference active power is considered constant to a specific optimal value calculated by the first optimization layer according to the different constraints mentioned above. The simulation results of the second optimization layer represent a comparison between the PEV_{AGi} dynamic response using conventional PI's parameters given in Table 4 and PI's gains estimated by the on-line multi objective PSO algorithm.

The four pairs regulator's gains of each PEV_{AGi} , pictured in Fig. 8, show a marked modification throughout the up and down loads demands and the injected or absorbed PEV_{AGi} active power variations. These gains are self-adjusted to minimize, the most possible, the error between the measured values and their corresponding reference of the optimized PEV_{AGi} 's DC bus voltage, battery current and G2V/V2G current in both axes d,q. The on-line multi objective PSO algorithm is ceased of execution when the inferior error is reached and hence the PEV_{AGi} response achieves its optimal functionality point to guarantee the maximum PEV_{AGi} performance and efficiency in ancillary services participating.

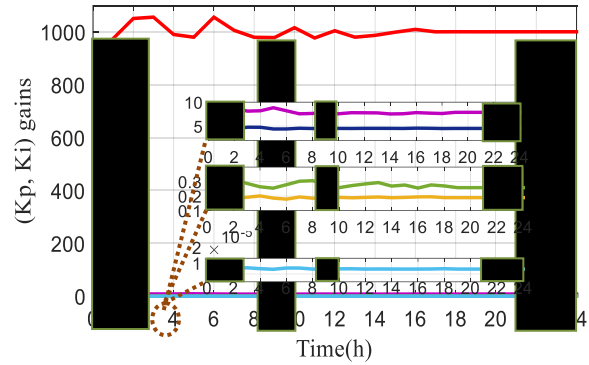


Fig. 8. (k_p, k_i) PI regulators' parameters for: Battery current, DC link voltage, G2V/V2G currents using second optimization layer based on-line multi-objective PSO algorithm.

The results in Fig. 9 show the dynamics of the PEV_{AG1} , PEV_{AG2} and PEV_{AG3} batteries current during their participation in the ancillary services. These results confirm the elected convention in which the negative currents correspond to the G2V concept and the positive currents correspond to the V2G concept. According to this figure, the curve using the conventional regulators presents a mediocre solution since it has large oscillations and slow stabilization. On the other hand, the curve using the second optimization layers shows that the current pursue, rapidly, its reference with little perturbations during different operating states transitions.

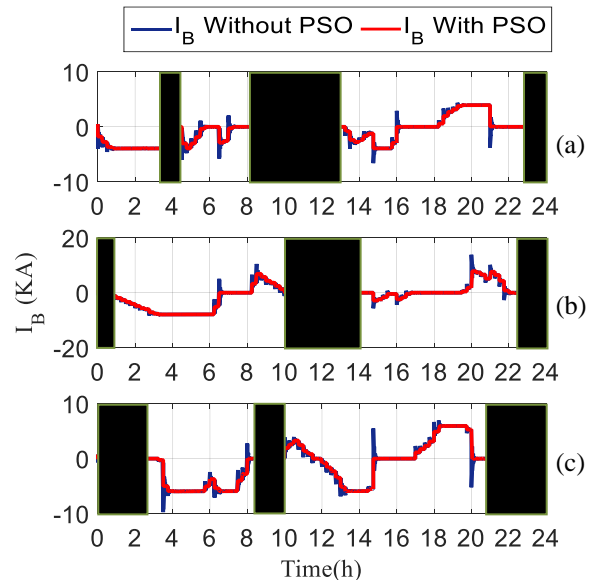
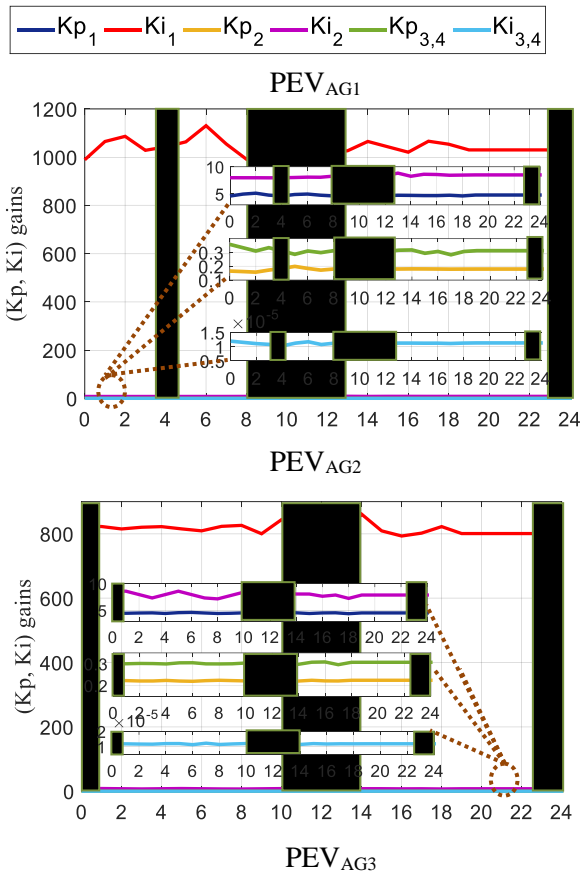


Fig. 9. Profiles of each PEV_{AGi} battery current: (a) For PEV_{AG1} . (b) For PEV_{AG2} . (c) For PEV_{AG3} .

Fig. 10 illustrates the DC bus voltage behavior using the conventional and the on-line optimized PI's gains. It is observable that the oscillation and the settling time are more minimized within the on-line adjusting PI's parameters. The system stability and the convergence to the reference value after every disturbance is ensured more quickly than the conventional method. In fact, the second optimization layers

launch a [finding](#) for a novel regulator gain to correlate the PEV_{AGi}'s DC bus voltage to its reference value during every system's change statement.

Fig. 10. Profiles of each PEV_{AGi} DC bus voltage: (a) For PEV_{AG1}. (b) For PEV_{AG2}. (c) For PEV_{AG3}.

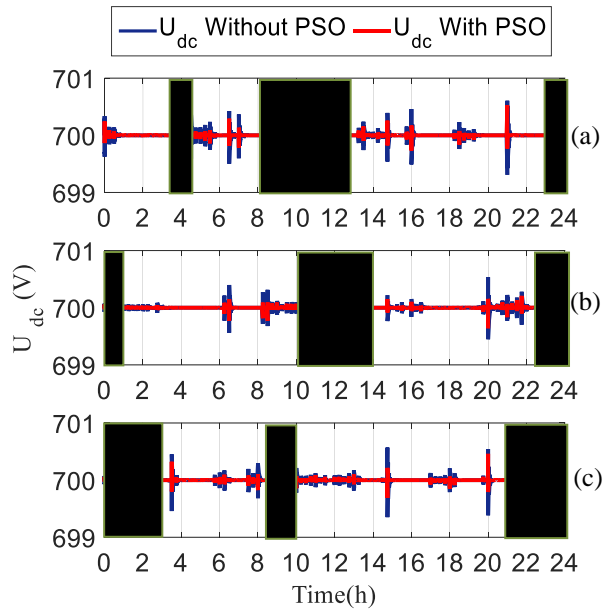


Table3

PSO parameters values for both optimization layers.

PSO parameters	First optimization layer	Second optimization layer
Population size	1000	50
Number of Iterations	40	20
Inertia weight W	1	1
Acceleration coefficients (C1,C2)	(2,2)	(2,2)

Table4

PSO and conventional PI controllers' specifications.

PI regulators	PI gains of PEV _{AGi} battery current		PI gains margin of PEV _{AGi} DC bus voltage		PI gains margin of PEV _{AGi} G2V/V2G current in d,q axes	
Parameters	Kp ₁	Ki ₁	Kp ₂	Ki ₂	Kp _{3,4}	Ki _{3,4}
Range of each PI parameter with PSO	[0 50]	[400 2000]	[0 10]	[0 100]	[0 5]	[0 20]
conventional PI parameter	2.2359	237.15	0.1556	5.5	5e-5	5

Fig .11 shows the power curves transferred between the grid and the PEV_{AGi} over the 24-h. The negative powers present the charge operation and the positive powers affirm the operation of the discharge. The overshoots are mitigated in PSO method as the conventional method. This figure shows the importance of the second optimization layer. In fact, absolute PEV_{AGi} real powers followed their references calculated by the first optimization, which is ensured using the corresponding gains found by the adapted PSO algorithm.



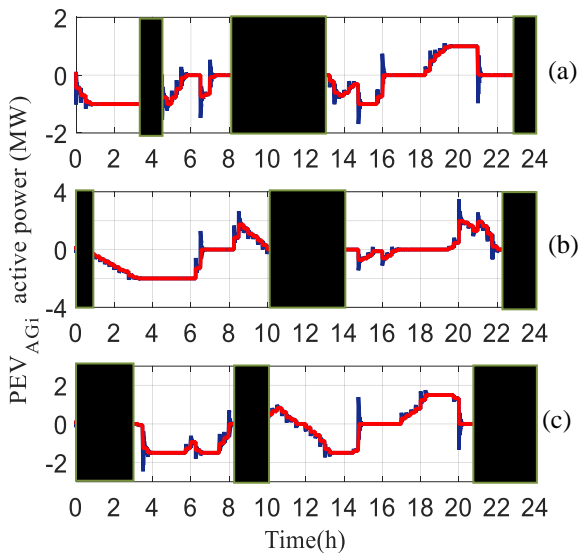


Fig. 11. Profiles of each PEV_{AGi} absorbed or injected active power: (a) For PEV_{AG1} . (b) For PEV_{AG2} . (c) For PEV_{AG3} .

These gains are flexible since each new system state has different regulators coefficients not similar to those already found before. And hence, a perfect PEVs injection and absorption is ensured. It is also clear that using first layer optimization layers with classical PI controllers is not satisfactory due to the response delay, the oscillations and deficiency of accuracy tracking. On the other hand, the use of the two optimizations layers of "PEVCC" approach represents an adequate and robust solution.

The correct operation of the "PEVCC" approach and the constraints satisfactions can also be confirmed by the evolution of the SOC curve of each PEV_{AGi} battery as shown in Fig. 12. It is clear that at each PEV_{AGi} connection time to the smart grid, a new initial SOC value is detected to launch G2V or V2G operation. In addition, it is also observable, that the SOC curves during one day and during the various operating states are well understood between the maximum and minimum battery SOC boundary with the use of optimized regulators than a conventional one.

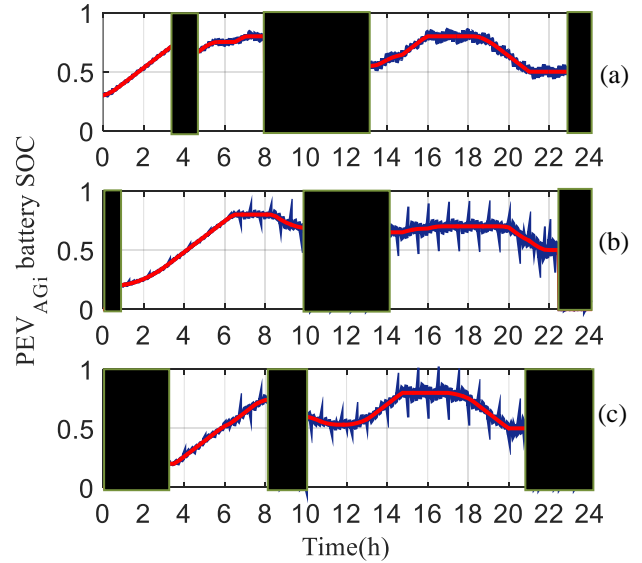


Fig. 12. Profiles of each PEV_{AGi} battery SOC: (a) For PEV_{AG1} . (b) For PEV_{AG2} . (c) For PEV_{AG3} .

4.3. Simulation results of PEVCC objectives attainments:

The improvement of the proposed "PEVCC" approach on daily power demands smoothness for one day can be summarized in Fig. 13. It is observable that this power can be greatly flattened. Indeed, the power curve of the total load demands using the first and second optimization layers, shown in red, is more performant and robust than the other curves corresponding to the first optimization layer with convention PI regulators and without "PEVCC" intervention presented in blue and green curve, respectively. Moreover, it is perceptible that the red curve is generally enhanced within the optimal ranges of loads demands. However, sometimes the total load demands curve remains unchanged if the PEVs are not connected or for some constraints like unsuitable electricity price or SOC limits attainments as shown in these periods [8-8.15h], [11.30-12 h], [16.45-17h] and [22-0h].

Fig. 14 shows the behaviors of the grid frequency within the first and second optimization layers, the first optimization layer with convention PI regulators and without "PEVCC" intervention presented in red, blue and green curves, respectively. It is observable that the frequency state before regulation is fluctuated. It exceeds the exigencies set by the standards. For the other two curves, shown in zooms, they are acceptable and meet the criterion's requirements. Except for that, the red curve corresponding to optimized controllers is the best since it has high performance and robustness at different state variations.

— SOC Without PSO — SOC With PSO

— P_L^t With both optimization layers — Initial P_L^t P_L^t With first optimization layer

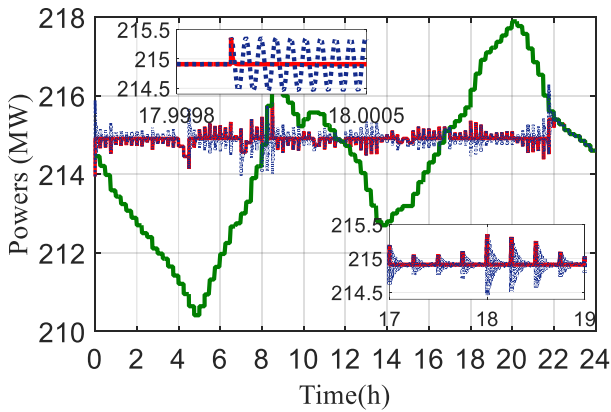


Fig. 13. Daily loads demands behavior with "PEVCC" approach.

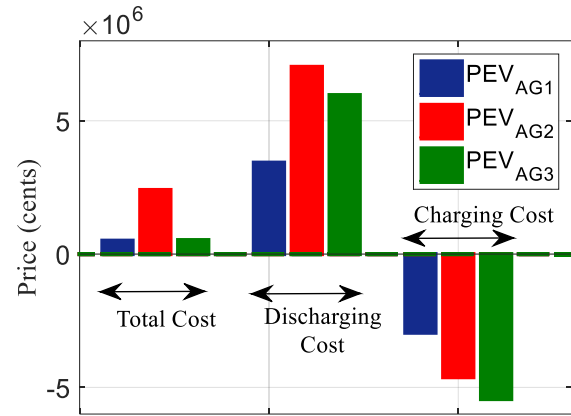


Fig. 15. Total cost behavior of each PEV_{AGi} owners with "PEVCC" approach.

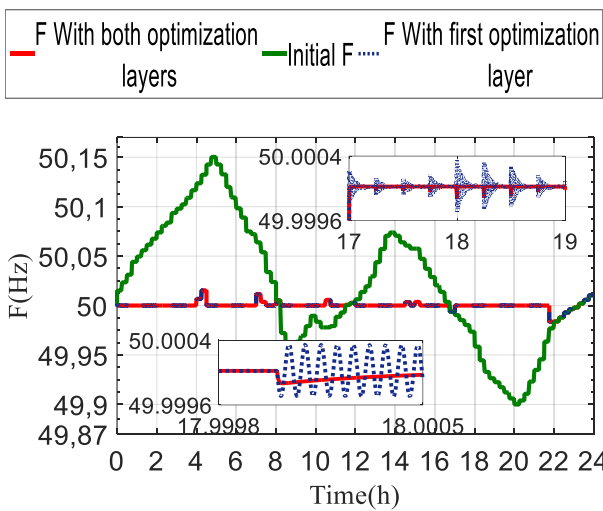


Fig. 14. Grid frequency behavior with "PEVCC" approach.

The monetary benefit of each PEV_{AGi} owner from using the proposed "PEVCC" approach to participate in the electricity market is illustrated in Fig. 15. This benefit is the difference between the power purchased during G2V operation and the power sold during V2G operation. It is noted that during these periods [8-8.15h], [11.30-12h], [16.45-17h] and [22-0h], neither selling nor buying is insured due to limits SOC attainment of PEV's batteries or not to PEV plunged to post charge or to expensive electricity price with G2V concept or to cheaper electricity price with V2G concept. Conventionally, the PEVs are connected to the post charge only for charging at any electricity price, so PEV user will only buy powers. But now with the exploitation of proposed approach, PEVs are, optimally, integrated into distribution systems not only to improve the reliability of the smart grid, but also to raise revenue and money earn to PEVs users.

4.4. Discussion results

In this section a comparison between the results obtained by proposed "PEVCC" strategy and the existing results of literature is ensured. In fact, the study in [37], focusing on minimization of PEV battery charging energy cost, proves by simulation results the performance of V2G operation during the high price energy to give economic returns and money earn to PEV users. Moreover, another study in [38], focusing on frequency regulation, proves by simulation results the reduction of frequency deviation against load changes by keeping the equilibrium between loads power demands and grid power generation. Also, the work in [39], focusing on daily power demand smoothness in smart grid, proves, by experimental results, the ability of PEV with its both V2G and G2V operation concepts to ensure a flattened power load curve in a residential application. All these methods have proposed good solutions to enhance power electrical system quality. However, each of them focuses on a specific objective task, and they don't take into account various problems in power systems. It is also noted, that these methods don't favor enough flexibility either in PEV duration of charging or in time of connection and disconnection. Moreover, they don't consider PEV battery's lifetime improvement during participating in the ancillary services. Compared to present studies, the proposed study joins all these techniques on one control strategy to solve, at the same time, various problems in the electrical network. In fact, the proposed control strategy favors both interaction and electrical power flow exchange between PEVs and smart grid in order to ensure, simultaneously with big flexibility in PEV time connection or disconnection: the regulation of grid frequency as shown in Fig. 14, achievement of the smart grid daily power demand smoothness as illustrated in Fig. 13, the minimization of daily total cost incurred for each PEV charging/discharging as described in Fig. 15, the detection of optimal operating access of V2G or G2V concepts as mentioned in Fig. 11, the control of battery SOC

for each PEV as shown in Fig. 12 and the achievement of optimal PEVs dynamic responses by adjusting all their regulators parameters during participating in these mentioned ancillary services as presented in Fig. 8.

5. Conclusion

In this paper, a novel multi-objective "PEVCC" strategy has been proposed for the optimal integration of PEVs into the smart grid in order to solve various problems quality in power systems and participate in the electricity market at the same time. The proposed "PEVCC" strategy could be generalized in any smart grid with any number of PEVs. Besides, it considers as a maximum, the flexibility in PEV joining or disjoining time to post charge. This strategy is generally composed of two optimization levels: The purpose of the first one is to estimate the optimal reference power applied to each connected PEV's converter to reach, simultaneously, the maximization of grid frequency quality enhancement, the minimization of the daily power demand variance, the minimization of charging energy cost to give economic returns to PEV users, the detection of PEV optimal operating access to function in V2G or G2V concepts and the control of each PEV battery SOC limits. The second optimization level is concentrated on ameliorating the PEV dynamic responses by self-adjusting all its regulators gains using the on-line multi-objective PSO algorithm during different PEV ancillary services participating. The software results show that variations in the total daily load and the grid frequency are considerably reduced in desired ranges as well as to the economic returns given to the PEVs users. This proves the efficiency of the proposed control and its ability to optimally integrate PEVs into the smart grid .

References

- [1] S. Essallah, A. Khedher, A. Bouallegue, "Integration of distributed generation in electrical grid: Optimal placement and sizing under different load conditions", *Computers and Electrical Engineering*, vol. 79, pp. 106461, 2019.
- [2] X. Lu, K. Zhou, X. Zhang, S. Yang, "A systematic review of supply and demand side optimal load scheduling in a smart grid environment", *Journal of Cleaner Production*, vol. 203, pp. 757-768, 2018.
- [3] Y. Fu, X. Zhang, Y. Hei, H. Wang, "Active participation of variable speed wind turbine in inertial and primary frequency regulations", *Electric Power Systems Research*, vol. 147, pp. 174-184, 2017.
- [4] A.M. Howlader, S. Sadoyama, L.R. Roose, S. Sepasi, "Distributed voltage regulation using Volt-Var controls of a smart PV inverter in a smart grid: An experimental study", *Renewable Energy*, vol. 127, pp. 145-157, 2018.
- [5] A.Q. Al-Shetwi, M.A. Hannan, K.P. Jern, M. Mansur, T.M.I. Mahlia, "Grid-connected renewable energy sources: Review of the recent integration requirements and control methods", *Journal of Cleaner Production*, vol. 253, pp. 119831, 2020.
- [6] N. Mararakanye, B. Bekker, "Renewable energy integration impacts within the context of generator type, penetration level and grid characteristics", *Renewable and Sustainable Energy Reviews*, vol. 108, pp. 441-451, 2019.
- [7] W.J. Requia, M. Mohamed, C.D. Higgins, A. Arain, M. Ferguson, "How clean are electric vehicles? Evidence-based review of the effects of electric mobility on air pollutants, greenhouse gas emissions and human health", *Atmospheric Environment*, vol. 185, pp. 64-77, 2018.
- [8] A.C.R. Teixeira, J.R. Sodr e, "Impacts of replacement of engine powered vehicles by electric vehicles on energy consumption and CO2 emissions", *Transportation Research Part D*, vol. 59, pp. 375-384, 2018.
- [9] R. . Fern andez, "A more realistic approach to electric vehicle contribution to greenhouse gas emissions in the city", *Journal of Cleaner Production*, vol. 172, pp. 949-959, 2018.
- [10] H. Liu, K. Huang, N. Wang, J. Q. Q. Wu, S. Ma, C. Li, "Optimal dispatch for participation of electric vehicles in frequency regulation based on area control error and area regulation requirement", *Applied Energy*, vol. 240, pp. 46-55, 2019.
- [11] M.F.M. Arani, Y.A.R.I. Mohamed, "Cooperative Control of Wind Power Generator and Electric Vehicles for Microgrid Primary Frequency Regulation", *IEEE Transactions on Smart Grid*, vol. 9, pp. 5677-5686, 2018.
- [12] Y. Li, L. Li, C. Peng, J. Zou, "An MPC based optimized control approach for EV-based voltage regulation", *Electric Power Systems Research*, vol. 172, pp. 152-160, 2019.
- [13] Y. Zheng, Y. Shang, Z. Shao, L. Jian, "A novel real-time scheduling strategy with near-linear complexity for integrating large-scale electric vehicles into smart grid", *Applied Energy*, vol. 217, pp. 1-13, 2018.
- [14] S. Khemakhem, M. Rekik, L. Krichen, "A collaborative energy management among plug-in electric vehicle, smart homes and neighbors' interaction for residential power load profile smoothing", *Journal of Building Engineering*, vol. 27, pp. 100976, 2020.
- [15] Y. Shi, H.D. Tuan, A.V. Savkin, T.Q. Duong, H.V. Poor, "Model Predictive Control for Smart Grids with Multiple Electric-Vehicle Charging Stations *IEEE Transactions on Smart Grid*, vol. 10, pp. 2127-2136, 2019.
- [16] A. Ghasemi, S.S. Mortazavi, E. Mashhour, "Hourly demand response and battery energy storage for imbalance reduction of smart distribution company embedded with electric vehicles and wind farms", *Renewable Energy*, vol. 85, pp. 124-136, 2016.

- [17] S. Padhy, S. Panda, "A hybrid stochastic fractal search and pattern search technique based cascade PI-PD controller for automatic generation control of multisource power systems in presence of plug in electric vehicles", *CAAI Transactions on Intelligence Technology*, vol. 2, pp. 12-25, 2017.
- [18] A.K Yadav, P. Gaur, "An Optimized and Improved STF-PID Speed Control of Throttle Controlled HEV", *Arabian Journal for Science and Engineering*, vol. 41, pp. 3749-3760, 2016.
- [19] Y. Yan, Y. Qian, H. Sharif, D. Tipp, "A Survey on Smart Grid Communication Infrastructures: Motivations, Requirements and Challenges", *IEEE Communications Surveys & Tutorials*, vol. 15, pp. 5-20, 2013.
- [20] Y. Kabalci, "A survey on smart metering and smart grid communication", *Renewable and Sustainable Energy Reviews*, vol. 57, pp. 302-318, 2016.
- [21] G. William Chugulu, F. Simba, S. Lujara, "Proposed Practical Communication Architecture for Automatic Fault Detection and Clearance in Secondary Distribution Power Network", *International Journal of Smart Grid*, vol. 4, pp. 165-175, 2020.
- [22] A. Al Khas, I. Cicek, "SHA-512 based Wireless Authentication Scheme for Smart Battery Management Systems", *International Journal of Smart Grid*, vol. 4, pp. 12-16, 2020.
- [23] X. Li, Z. Wang, L. Zhang, "Co-estimation of capacity and state-of-charge for lithium-ion batteries in electric vehicles", *Energy*, vol. 174, pp. 33-44, 2019.
- [24] L. Zhang, H. Peng, Z. Ning, Z. Mu, C. Sun, "Comparative Research on RC Equivalent Circuit Models for Lithium-Ion Batteries of Electric Vehicles", *Applied Sciences*, vol. 7, pp. 1002, 2017.
- [25] K. Dehghanpour, S. Afsharnia, "Electrical demand side contribution to frequency control in power systems: a review on technical aspects", *Renewable and Sustainable Energy Reviews*, vol. 41, pp. 1267-1276, 2015.
- [26] C. Zhao, U. Topcu, N. Li, S. Low, "Design and Stability of Load-Side Primary Frequency Control in Power Systems", *IEEE Transactions on Automatic Control*, vol. 59, pp. 1177-1189, 2014.
- [27] J.M. Guerrero, J.C. Vasquez, J. Matas, L.G de Vicuña, M. Castilla, "Hierarchical Control of Droop-Controlled AC and DC Microgrids - A General Approach Toward Standardization", *IEEE Transactions on Industrial Electronics*, vol. 58, pp. 158-172, 2011.
- [28] Y. Andegelile, H. Maziku, N. Mvungi, M. Kissaka, "Software Defined Communication Network Reliability for Secondary Distribution Power Grid", *International Journal of Smart Grid*, vol. 4, pp. 118-124, 2020.
- [29] T. Harighi, R. Bayindir, E. Hossain, "Overviewing Quality of Electric Vehicle Charging Stations' Service Evaluation", *International Journal of Smart Grid*, vol. 2, pp. 41-48, 2018.
- [30] Y. Niewa, Y. Zhang, Y. Zhao, B. Fang, L. Zhang, "Wide-area optimal damping control for power systems based on the ITAE criterion", *Electrical Power and Energy Systems*, vol. 106, pp. 192-200, 2019.
- [31] L. Hu, F. Xue, Z. Qin, J. Shi, W. Qiao, W. Yang, T. Yang, "Sliding mode extremum seeking control based on improved invasive weed optimization for MPPT in wind energy conversion system", *Applied Energy*, vol. 248, pp. 567-575, 2019.
- [32] M. Chouket, A. Abdelkafi, L. Krichen, "Tuned Controller's Gain Tested under Grid Voltage Sags Using PSO Algorithm", *Journal of Electrical Power & Energy Systems*, vol. 2, pp. 6-18, 2018.
- [33] I. Darwich, I. Lachhab, L. Krichen, Implementation of an on-line multi-objective particle swarm optimization controllers gains self adjusted of FC/UC system devoted for electrical vehicle", *International Journal of Hydrogen Energy*, vol. 44, pp. 28262-28272, 2019.
- [34] N.K. Jain, U. Nangia, J. Jain, "A Review of Particle Swarm Optimization", *Journal of The Institution of Engineers (India): Series B*, vol. 99, pp. 407-411, 2018.
- [35] A. Khare, S. Rangnekar, "A review of particle swarm optimization and its applications in Solar Photovoltaic system", *Applied Soft Computing*, vol. 13, pp. 2997-3006, 2013.
- [36] A. Elrheem E.A. Mostafa, N. K. Bahgat, "A Comparison Between Using A Firefly Algorithm and A Modified PSO Technique for Stability Analysis of a PV System Connected to Grid", *International Journal of Smart Grid*, vol. 1, pp. 2-8, 2017.
- [37] Y. Dahmane, R. Chenouard, M. Ghanes, M. Alvarado-Ruiz, "Optimized time step for electric vehicle charging optimization considering cost and temperature", *Sustainable Energy, Grids and Networks*, vol. 26, pp. 100468, 2021.
- [38] M. Khan, H. Sun, Y. Xiang, D. Shi, "Electric vehicles participation in load frequency control based on mixed H₂/H_∞", *International Journal of Electrical Power & Energy Systems*, vol. 125, pp. 106420, 2021.
- [39] K. MiaoTan, V.K. Ramachandramurthy, J. YingYong, M. Tariq, "Experimental verification of a flexible vehicle-to-grid charger for power grid load variance reduction", *Energy*, vol. 228, pp. 120560, 2021.